Complexation of Naphthylethanols with β-Cyclodextrin

T. C. Barros,[1a] K. Stefaniak,[1a] J. F. Holzwarth,[1b] and C. Bohne*,[1a]

Department of Chemistry, University of Victoria, P.O. Box 3065, Victoria, BC, Canada V8W 3V6, and Fritz-Haber-Institut der Max-Planck Gesellshaft, Faradayweg 4-6, 14195 Berlin, Germany

Received: December 2, 1997; In Final Form: February 13, 1998

The complexation behavior of 1-naphthyl-1-ethanol (1-NpOH) and 2-naphthyl-1-ethanol (2-NpOH) with β-cyclodextrin (β-CD) was studied by employing several spectroscopic techniques. In the case of 1-NpOH, only a complex with 1:1 stoichiometry is formed with β-CD, which has an equilibrium constant that is smaller than that observed for the 1:1 complex between β-CD and 2-NpOH. Excimer emission was observed in the presence of β-CD for solutions containing high 2-NpOH concentrations. This excimer emission was ascribed to a complex with 2:2 β-CD/2-NpOH stoichiometry. In addition, ^{1}H NMR data suggest that 2-NpOH is axially incorporated into the β-CD cavity. Only in the case of 2-NpOH was a broadening of the signals corresponding to the aromatic protons observed in the presence of β-CD. This broadening was attributed to the formation of the 2:2 complex. The dynamics of NpOH complexation was investigated by using the quenching methodology for triplet states. The entry rate constants for the 1:1 complex of 1-NpOH and 2-NpOH are $(4.7 \pm 1.9) \times 10^8$ M^{-1} s^{-1} and $(2.9 \pm 1.6) \times 10^8$ M^{-1} s^{-1}, respectively, whereas the exit rate constants for the two compounds are $(4.8 \pm 1.8) \times 10^5$ s^{-1} and $(1.8 \pm 0.7) \times 10^5$ s^{-1}. In the case of 2-NpOH, we were able for the first time to estimate the rate constant for the dissociation of a β-CD 2:2 complex ($(0.2-2.5) \times 10^3$ s^{-1}), showing that the dynamics for complexes including more than one cyclodextrin are remarkably slower than the dynamics observed for 1:1 complexes.

Introduction

Cyclodextrins (CDs) are cyclic oligosaccharides with 6 (α), 7 (β), or 8 (γ) D-glucose units, which have a relatively hydrophobic cavity for guest binding. Cyclodextrins provide a chiral environment which is mainly defined by the primary and secondary alcohol groups located at the narrower and wider entrances of the cavity, respectively. These compounds have been extensively employed to understand host−guest complexation, to develop sensors for binding, and as mimetic systems for enzyme reactivity.[2−6] The versatility of cyclodextrins as hosts is related to the fact that different cavity sizes are readily available and functionalization of one or many alcohol moieties is possible.[7,8]

A variety of organic or inorganic molecules are included in the fairly hydrophobic cavity of cyclodextrins.[9−11] Relatively weak forces, such as van der Waals forces, dipole−dipole interactions, and hydrogen bonds, as well as size complementarity, i.e., how well guests fit inside the cavity, determine the efficiency for complexation. Equilibrium constants have been directly determined from calorimetric methods or indirectly from spectroscopic measurements. In the latter case, a spectroscopic property of the guest or cyclodextrin has to change when the complex is formed, and equilibrium constant values are obtained by analyzing the magnitude of the changes with cyclodextrin concentrations.[12] UV−vis absorption, fluorescence, conductimetry, and ^{1}H NMR have been employed in many cases.[13,14] Some of these techniques can provide additional information on the structure of the complex. For example, fluorescence can be frequently related to the polarity of the microenvironment[15] or ^{1}H NMR provides information of the location of the guest within the cyclodextrin cavity.[16−18] Cyclodextrins can form complexes with different guest to host stoichiometries. Most frequently the complexes have 1:1 guest/CD stoichiometries. However, 1:2 and 2:2 complexes have been found, particularly when the guest is too large and part of it is not completely included in the cavity.

Polycyclic aromatic hydrocarbons bind to cyclodextrins, and the size of the aromatic ring determines which type of cyclodextrin will form stronger complexes. In general, benzene derivatives bind efficiently to α-CD and naphthalenes to the larger β-CD. The binding of naphthalene and its derivatives has been extensively studied.[11,19−27] The average equilibrium constant for naphthalene complexation with β-CD derived from several studies is (730 ± 120) M^{-1}. In most of these studies a 1:1 complexation stoichiometry was assumed. However, on the basis of the observation of excimer emission it was established that a 2:2 naphthalene/β-CD is also formed with an equilibrium constant of 4000 M^{-1}.[19] Indeed, excimer emission due to the incorporation of two chromophores in the cyclodextrin complexes has been observed for a variety of naphthalene derivatives.[19,22,26,27] The 1:1 equilibrium constants of naphthalenes substituted at the 2-position with β-CD are in general similar to those observed for naphthalene,[11,22,23,27] but a much larger value was observed for 2,3-dimethylnaphthalene (2600 M^{-1}).[25] Substitution at the naphthalene 1-position leads to lower equilibrium constants when compared to naphthalenes substituted at the 2-position. From circular dichroism spectra it was determined that substitution at the 2-position leads to incorporation along the long axis of naphthalene, whereas 1-substituted naphthalenes have different modes of inclusion, probably due to the steric interactions of the substituent with the cyclodextrin.[28]

The magnitude of equilibrium constants provide information on the complexation efficiency. However, they do not provide any information on the entry/exit dynamics for the guest with the cyclodextrin. Understanding of this complexation dynamics

S1089-5639(98)00384-3 CCC: $15.00
Published on Web 04/17/1998

is important when these host−guest complexes are designed to perform functions such as catalysis or transport. There is much less information available on the cyclodextrin complexation dynamics than on the complexation efficiency.[29] This situation is probably due to the fact that most entry/exit processes are fast and can only be studied with fast kinetic techniques. Furthermore, the dynamics of complexation cannot be extrapolated from the magnitude of equilibrium constant values. For example, the observation of small equilibrium constants does not indicate that the compounds do not interact with cyclodextrins but may signal that the entry and exit processes occur on similar time scales. This is the case for a series of salts where the equilibrium constants were smaller than 30 M^{-1}, but the entry and exit processes, determined by ultrasonic relaxation, were quite fast ($(0.4-20) \times 10^8$ M^{-1} s^{-1} and $(0.4-7) \times 10^7$ s^{-1}).[30]

Photophysical techniques are suitable to probe the mobility in the nano- to microsecond time domain, because the lifetime of excited state probes is of the same order of magnitude as the dynamic processes of interest. With most guest molecules the entry/exit rate constants cannot be obtained by direct kinetic measurements, and a quenching methodology is employed, where an aqueous quencher primarily interacts with the probe free in solution.[29] The entry and exit rate constants can be obtained by analyzing the change in the probe's triplet lifetime at increasing quencher concentrations. This method was employed to study the complexation dynamics of naphthalene and its derivatives with cyclodextrins.[20,24,31] In the case of xanthone, the entry and exit rate constants of triplet xanthone with β-CD can be obtained from direct kinetic analysis of the triplet decay.[32,33] This analysis lead to a much smaller equilibrium constant for the triplet state when compared to that for the ground state. The exit rate constant for triplet xanthone can be slowed when alcohols are present in solution,[34] showing that the exit process is very sensitive to the environment in the host−guest complex.

The original motivation for this work was to establish if chiral discrimination could be observed for the complexation dynamics of the enantiomers of 1-naphthyl-1-ethanol (1-NpOH) and

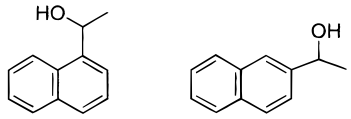

1-NpOH **2-NpOH**

2-naphthyl-1-ethanol (2-NpOH) with β-CD. We were not able to accomplish this objective due to the large errors associated with the recovered rate constants. However, during the development of the project the formation of the 2:2 complex for 2-NpOH and β-CD was established, which showed to have a very interesting complexation dynamics. For this reason, our objective was redefined to compare the complexation efficiencies and dynamics of 1-NpOH with that of 2-NpOH, since for the former no 2:2 complex was observed. In addition, we combined photophysical studies, i.e., fluorescence and laser flash photolysis, with ^{1}H NMR studies in order to obtain more insight into the dynamics of cyclodextrin complexation.

Experimental Section

Materials. The β-CD sample was a generous gift from Cerestar (lots C6 034-13 and F6080-191) and was used without further purification. β-CD from Merck was employed for a few of the calorimetry experiments. (*R*)-, (*S*)-, and (±)-1-naphthyl-1-ethanol (Fluka), (*R*)-, (*S*)-, and (±)-2-naphthyl-1-ethanol (Fluka), $MnSO_4$ (BDH), Na_2SO_4 (BDH), $[Co(NH_3)_5Cl]Cl_2$ (supplied by Dr. A. D. Kirk, University of Victoria), D_2O (Cambridge Isotope Laboratories or Sigma), and methanol (spectroscopic grade, ACP Chemicals Inc.) were used as received. $NaNO_2$ (Aldrich) was recrystallized from water. Deionized water (SYBRON, Barnstead, or Millipore deionizing systems) was employed for all samples.

Equipment. UV−vis absorption spectra were recorded using a Cary 5 or Cary 1 from Varian or a Shimadzu 2100 spectrophotometers. A PTI QM-2 fluorometer was employed to measure steady-state fluorescence spectra (20.0 ± 0.5 °C). The excitation and emission slit widths were set to obtain a band-pass between 2.0 and 3.0 nm, and the excitation wavelength was 280 nm. Lifetimes were measured with a PTI LS-1 time-correlated single photon counter (20.0 ± 0.5 °C). Water containing ground silica gel was employed as the scatterer to obtain the instrument response function (IRF). The excitation wavelength was 280 nm, and the emission was recorded at 330 nm. Visual analysis of the residuals, the autocorrelation function, and evaluation of χ^2 values were used as criteria for the goodness of fit.

Laser flash photolysis[34] was employed to measure the triplet−triplet absorption spectra and decay kinetics at 20 ± 2 °C. Samples were excited either with an excimer (308 nm) or a YAG laser (266 nm). Naphthalenes in aqueous solution are easily photoionized through a two-photon process. This photoionization can be minimized by attenuation of the laser energy (≤20 mJ/pulse). The contribution of photoionization was checked before every experiment by measuring the absorption for solvated electrons at 680 nm. A nonpulsed 150 W Xe-arc lamp (home-built lamp housing and Canrad Hanovia power supply) was employed to measure lifetimes longer than 4 μs. This lamp is suitable for measuring lifetimes in the order of hundreds of microseconds.

^{1}H NMR spectra were obtained with a 360 MHz spectrometer (Bruker AMX360). Chemical shifts were measured with respect to the residual water signal at $\delta = 4.65$ ppm.

A MicroCal ITC instrument was employed to perform isothermal titration calorimetry experiments. After filling of the reaction cell, positioning of the injector assembly, and initiation of stirring, the temperature was stabilized. A 250 μL syringe was employed for the following injection schedule: initial 1 min wait period followed by a 30 s injection of 10 μL and a subsequent wait period of 3 min between injections. Data were analyzed using the Origin (v. 2.9) for ITC analysis in Windows.[35]

Methods. *Preparation of Solutions.* NpOH aqueous solutions were prepared by injection of small volumes from a methanolic stock solution (ca. 10 mM). When required, the exact concentrations were determined from absorption spectra (1-NpOH, $\epsilon_{281} = 6250 \pm 242$ M^{-1} cm^{-1}; 2-NpOH, $\epsilon_{274} = 4680 \pm 35$ M^{-1} cm^{-1}; 2 independent determinations for each NpOH, each with at least 5 NpOH concentrations). Cyclodextrin stock solutions containing 10−12 mM β-CD were prepared by dissolving cyclodextrin in water or NpOH aqueous solutions, followed by at least 4 h of stirring. All solutions at lower β-CD concentrations were prepared by dilution.

For ^{1}H NMR experiments, solutions containing 0.3 mM of NpOH and 12 mM β-CD were prepared in D_2O. A small amount of the NpOH methanolic stock solution was placed in a volumetric flask, and methanol was evaporated with a gentle stream of nitrogen followed by the addition of D_2O. This NpOH

solution was employed to prepare the solutions containing β-CD which were stirred overnight.

For fluorescence experiments, we initially measured the spectra right after dilution of the concentrated β-CD stock solution, but we observed that more precise equilibrium constants were obtained when the solutions were stirred overnight. For time-resolved fluorescence measurements, oxygen was removed from the solutions by bubbling nitrogen for at least 20 min. Standard 10 mm × 10 mm quartz cells were employed.

Samples for laser flash photolysis experiments were prepared in the same way as for fluorescence and were contained in 7 mm × 7 mm Suprasil cells. In all cases, nitrogen was bubbled through the samples for at least 30 min in order to remove oxygen. Each sample was submitted to a maximum of 70 laser shots, to avoid any decomposition of NpOH due to photoionization. For this reason, multiple samples were used in the quenching experiments. The SO_4^{2-} concentration was kept constant at 0.5 M for the triplet quenching experiments with Mn^{2+}, by mixing appropriate amounts of two solutions containing the same NpOH and β-CD concentrations but 0.5 M of Na_2SO_4 or 0.5 M of $MnSO_4$. The salt concentration was not controlled for the quenching studies with $[Co(NH_3)_5Cl]^{2+}$ and $NaNO_2$, since the quencher concentrations were kept below 5 mM.

Calorimetry. The reaction cell and injection syringe contained 1.5 mL of a 0.2−0.3 mM solution of NpOH and 250 μL of a 10−12 mM β-CD solution, respectively. The exact concentrations of NpOH were determined by UV−vis spectroscopy.

Determination of Equilibrium Constants. The values for the equilibrium constants (K_{eq}) between NpOHs and β-CDs can be recovered from the analysis of the shift of the ^{1}H NMR resonance frequency of a particular proton ($\Delta\delta$) of NpOH or the change in its fluorescence intensity (ΔI). Assuming a 1:1 NpOH/CD stoichiometry and that the cyclodextrin concentration is always in excess over the NpOH concentration, the change in the observed parameter with cyclodextrin concentration is given by[12]

$$\Delta_{obs} = \frac{\Delta_x K_{eq}[CD]}{1 + K_{eq}[CD]} \quad (1)$$

where for ^{1}H NMR experiments Δ_{obs} and Δ_x correspond to $\Delta\delta$ and the maximum shift when all NpOH is complexed ($\Delta\delta_{max}$), respectively. In the case of fluorescence measurements, Δ_{obs} and Δ_x are related respectively to ΔI and a parameter that includes the difference in the fluorescence quantum yield of free and complexed NpOH and the total concentration of NpOH. Thus, for NMR studies the total concentration of NpOH does not have to be known, whereas for fluorescence measurements it is included in eq 1.

A linear relationship is obtained when eq 1 is plotted in a double-reciprocal fashion:

$$\frac{1}{\Delta_{obs}} = \frac{1}{\Delta_x} + \frac{1}{K_{eq}\Delta_x[CD]} \quad (2)$$

Equation 2 is frequently referred to as the Benesi−Hildebrand treatment,[36] and K_{eq} values can be recovered from this equation. However, when using eq 2, a high weight is given to the data with largest errors, i.e., for small Δ_{obs}. For this reason, we recovered the K_{eq} values from the nonlinear fit of the experimental data to eq 1 (Kaleidagraph software v.3.0). The double-reciprocal plots were employed to check for the validity of the assumption that the complexation stoichiometry was 1:1. A deviation from the linear relationship is observed if the incorrect stoichiometry is assumed.

In the case of 2-NpOH we observed the formation of complexes with 2:2 NpOH/CD stoichiometry in addition to the 1:1 complex (vide infra):

$$Np + CD \overset{K_1}{\rightleftharpoons} Np{-}CD \quad (3)$$

$$Np{-}CD + Np{-}CD \overset{K_2}{\rightleftharpoons} (Np{-}CD)_2 \quad (4)$$

The concentration of $(Np-CD)_2$ is given by[26]

$$[(Np-CD)_2] = \frac{[Np]_0 + [Np]_{aq} - K_1[CD]_0[Np]_{aq}}{2} \quad (5)$$

where the subscript "0" corresponds to total concentrations and the free 2-NpOH concentration ($[Np]_{aq}$) is given by

$$[Np]_{aq} = \frac{-(1 + K_1[CD]_0) + \sqrt{(1 + K_1[CD]_0)^2 + 8K_1^2K_2[CD]_0^2[NP]_0}}{4K_1^2K_2[CD]_0^2} \quad (6)$$

The change of the fluorescence intensity at a wavelength where only $(Np-CD)_2$ emits is directly related to the concentration of the 2:2 complex. Since the emission quantum yield of this species is not known, its absolute concentration cannot be determined. For this reason, we normalized the ΔI values at 12 mM β-CD to an arbitrary $(Np-CD)_2$ concentration of unity. The values for K_1 obtained at low 2-NpOH concentrations and the total concentrations of 2-NpOH and β-CD are known. The concentrations of $(Np-CD)_2$ were calculated for different K_2 values. The excimer concentration at 12 mM and changes in emission intensity were normalized to unity, since the excimer emission quantum yield is not known. The best K_2 value and its error were estimated by comparing the residuals between the calculated values for the 2:2 complex and the observed changes in emission intensity.

Determination of Entry and Exit Rate Constants. The complexation dynamics was measured for the triplet-excited state of NpOH (Scheme 1). To obtain the entry (k_+) and exit

SCHEME 1

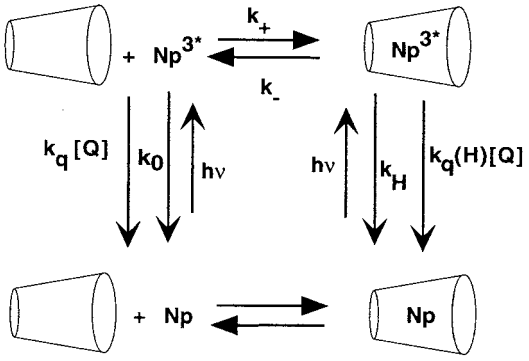

(k_-) rate constants, the triplet-excited-state lifetime has to be longer than the time associated with the dynamics of complexation. Since the triplet−triplet absorption spectra of free and complexed NpOH are the same, the quenching methodology was employed to recover the values for k_+ and k_- from the variation of the triplet decay rate constant (k_{obs}) with increasing quencher concentration.[20,29,37] When the triplet decay is first-

order at all quencher concentrations, the observed decay rate constant is given by

$$k_{obs} = k_H + k_- + k_q(H)[Q] - \frac{k_- k_+[CD]}{k_+[CD] + k_0 + k_q[Q]} \quad (7)$$

The values for the triplet lifetimes in the absence (k_0) and presence of β-CD (k_H) are known from experiments in the absence of quencher. These lifetimes are long (>30 μs) and are limited by small quantities of quenching impurities, such as oxygen. The values of k_0 and k_H employed for the fit of the experimental data to eq 7 varied slightly between experiments performed on different days. The quenching rate constants in aqueous solution (k_q) were determined from independent quenching plots ($k_{obs} = k_0 + k_q[Q]$). The three unknown parameters recovered from eq 7 are $k_q(H)$, k_+, and k_-. The precision with which one can recover these parameters depends on the difference between the quenching efficiencies for the probe in water and complexed to β-CD (k_q vs $k_q(H)$), as well as on the ratio between $k_+[CD]$ and k_-.[29] The latter relationship can be altered by varying the cyclodextrin concentration, and optimum curvature may be observed at intermediate host concentrations. For this reason, quenching experiments were performed at β-CD concentrations between 1 and 12 mM. The ideal situation with respect to the quenching efficiencies is when the difference between k_q and $k_q(H)$ is large. However when this is not the case, the recovered parameters have considerable errors, as observed in this study. To diminish these errors the values for $k_q(H)$ were estimated from the change of the initial slope of k_{obs} vs [Q] at different cyclodextrin concentrations. The derivative of eq 7 with respect to the quencher concentrations is given by

$$\frac{dk_{obs}}{d[Q]} = k_q(H) + \frac{k_q k_- k_+[CD]}{(k_+[CD] + k_0 + k_q[Q])^2} \quad (8)$$

Since $k_0 \ll k_+[CD]$ the initial slope ($[Q] \rightarrow 0$) is given by

$$\text{slope} = k_q(H) + \frac{k_q k_-}{k_+[CD]} \quad (9)$$

Quenching experiments were performed at different β-CD concentrations. The quenching plots were analyzed by the following procedure:

(1) For each β-CD concentration the data were fitted to eq 7. The recovered parameters for k_+, k_-, and $k_q(H)$ in general had large errors (50−100%). For this reason, this procedure only established the order of magnitude for each parameter.

(2) The data were plotted according to eq 9, and the values for $k_q(H)$ were determined from the intercept of the plot. The errors for this parameter were much smaller than for the free fit.

(3) The value for $k_q(H)$ obtained from eq 9 was fixed in eq 7. The k_+ values were varied between 8×10^7 and 2×10^9 M^{-1} s^{-1}, since the k_+ values recovered from procedure 1 fall within this interval. The values for k_- were determined from the fit to eq 7 at different fixed k_+ values. The values for k_+ and k_- were estimated from fits which did not deviate considerably from the experimental data, specially at low quencher concentrations where most of the curvature predicted by eq 7 occurs.

Results

Determination of Equilibrium Constants. Many guest molecules are not very soluble in water, and fluorometry, due to its sensitivity, is one of the few techniques that can be employed to determine equilibrium constants. Since NpOHs are relatively soluble in water, they provided an opportunity to compare different techniques for the determination of equilibrium constants. ^{1}H NMR, fluorometry, and calorimetry were used to determine the equilibrium constants for the enantiomers of 1-NpOH or 2-NpOH with β-CD.

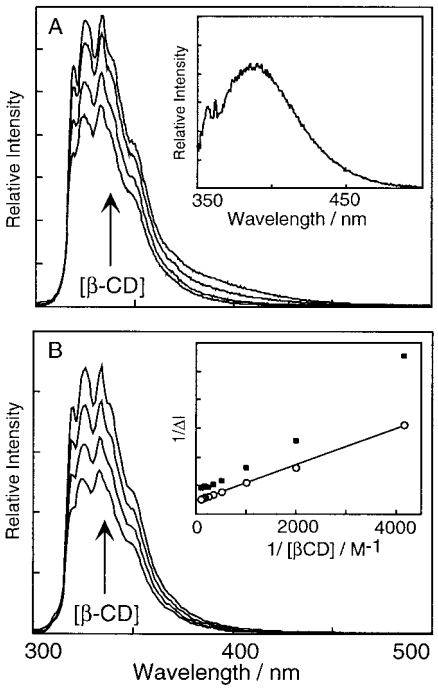

Figure 1. Increase of the fluorescence intensity of (*R*)-2-NpOH (A, 150 μM; B, 10 μM) in the presence of β-CD (0−10 mM). The inset in (A) shows the excimer emission spectrum obtained by subtraction of the spectra normalized at 333 nm in the absence and presence of 10 mM β-CD. The inset in (B) shows the double-reciprocal plots for the change in emission intensity with β-CD concentration for 150 μM (■) and (○) 10 μM (*R*)-2-NpOH.

Absorption and fluorescence have frequently been employed to determine equilibrium constants. Only very small changes were observed in the absorption spectra for both NpOHs in the presence of β-CD, and this technique could not be employed to determine the values for K_{eq}. However, a substantial increase was observed for the fluorescence intensity when the NpOHs were complexed to β-CD (Figure 1). The NpOH fluorescence lifetimes in the absence and presence of β-CD were also measured. The fluorescence decays in water are monoexponentials, and the singlet-excited lifetimes were 24 and 25 ns for 1-NpOH and 2-NpOH, respectively. In the presence of β-CD, a lengthening of the lifetimes was observed, and the decays were nonexponential. When one lifetime was fixed to the values determined in water, the lifetime values for the longer component were 34 and 37 ns for 1-NpOH and 2-NpOH, respectively. The preexponential factor for the longer lifetime increased at higher cyclodextrin concentrations, showing that this species corresponds to the NpOHs complexed to β-CD. Indeed, this increase in the lifetime is responsible for the intensity increase observed in the steady-state spectra (Figure 1).

Equilibrium constant for 1-NpOH enantiomers (150 μM) were determined from the variation of the emission intensity at 324 or 337 nm with β-CD concentration (1−12 mM) (Table 1).[38] The double-reciprocal plots were linear indicating that the complexation stoichiometry corresponds to a 1:1 ratio.

TABLE 1: Equilibrium Constants Determined by Fluorometry[a]

	$K_{eq}/10^3$ M^{-1}		
compd	1:1 complex	1:1 complex with 0.5 M Na_2SO_4	2:2 complex
(*R*)-1-NpOH	0.18 ± 0.01 (4)	0.53 ± 0.05 (1)	
(*S*)-1-NpOH	0.14 + 0.04 (4)	0.46 ± 0.08 (1)	
(*R*)-2-NpOH	0.78 ± 0.02 (2)	1.8 ± 0.2 (1)	3 ± 1[b]
(*S*)-2-NpOH	0.81 ± 0.01 (2)	1.7 ± 0.2 (1)	3 ± 1[b]

[a] The numbers in parentheses indicate the number of independent experiments; errors correspond to standard deviations for experiments performed more than once. For experiments performed once the errors correspond to the statistical deviations recovered from the fit to eq 1. [b] Errors were estimated from fits with different K_2 values (see Experimental Section).

The fluorescence spectra for 2-NpOH in the presence of β-CD are dependent on the 2-NpOH concentration. At 150 μM a new emission centered around 390 nm appears (inset Figure 1A), which corresponds to the emission of naphthalene excimers,[39−41] indicating that a complex with two 2-NpOH molecules is formed. The β-CD cavity is too small to hold two molecules of 2-NpOH. For this reason, the excimer emission comes from a 2:2 β-CD/2-NpOH complex. These types of complexes have been reported for several naphthalene derivatives.[19,22,26,27] At low 2-NpOH concentrations (10 μM) the excimer emission is not observed. The equilibrium constant for the 1:1 complex (K_1) was determined at these low concentrations by measuring the intensity increase at 324 or 333 nm (Table 1). The double-reciprocal plot for 10 μM 2-NpOH is linear (inset Figure 1B), suggesting that only the 1:1 complex was present. In contrast, the double-reciprocal plot for 150 μM of 2-NpOH is not linear due to the contribution of the 2:2 complex. The formation of excimers diminishes the values for ΔI for the monomer emission at high β-CD concentrations, and a fit of the experimental data assuming a 1:1 complex leads to higher values for K_1 than observed at low 2-NpOH concentrations.

To obtain the equilibrium constant values for the 2:2 complex (eq 4), the emission intensity was measured at 405 nm and a normalized excimer concentration was calculated from eq 5 using the K_1 value of 830 M^{-1} determined at low 2-NpOH concentrations. Adequate fits for the calculated concentrations with the change in the emission intensity for the excimer were obtained with a relatively wide range of K_2 values, leading to considerable uncertainties (Table 1).[42] Nevertheless, the values for K_2 indicate that the formation of the 2:2 complex is quite efficient. At 150 μM 2-NpOH and 10 mM β-CD the fraction of 2-NpOH free in solution and complexed in 1:1 and 2:2 complexes are 0.08, 0.60, and 0.32, respectively. In contrast, when the 2-NpOH concentration is decreased to 10 μM the same fractions are 0.11, 0.85, and 0.04.

The triplet quenching methodology which was employed to determine the dynamics of complexation required the use of high Mn^{2+} concentrations (see below). For this reason, we determined the equilibrium constants for 1-NpOH and 2-NpOH with β-CD in the presence of 0.5 M Na_2SO_4. The same behavior regarding the formation of excimers was observed for 2-NpOH in the absence and presence of salt. The same conditions described above were employed to determine the equilibrium constants in the presence of Na_2SO_4. A significant increase was observed for the equilibrium constants related to the 1:1 complexes of 1-NpOH and 2-NpOH (Table 1). In contrast, when the increase of the excimer emission intensity was related to the normalized excimer concentration using a value for K_1 of 1.8×10^3 M^{-1}, the recovered value for K_2 was the same as in the absence of salt (3×10^3 M^{-1}).

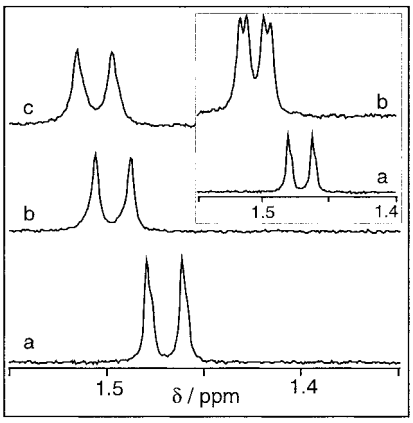

Figure 2. ^{1}H NMR for the methyl signal of (*R*)-1-NpOH (0.3 mM) in D_2O in the absence (a) or presence of 5 mM (b) and 12 mM (c) β-CD. The inset shows the NMR for (±)-1-NpOH in D_2O in the absence (a) and presence (b) of 12 mM β-CD.

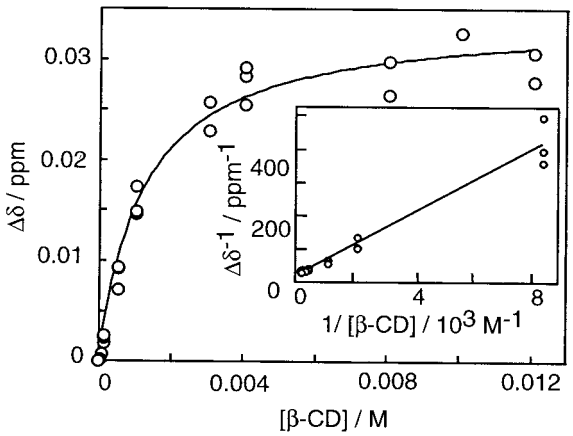

Figure 3. Dependence of the change in chemical shift for the signal corresponding to the (*R*)-2-NpOH methyl protons with β-CD concentration. Data for 3 independent experiments are shown. The inset shows the double-reciprocal plot.

The ^{1}H NMR signals for NpOH and β-CD shift when the complex is formed. Equilibrium constants were determined by analyzing the change in the signal which corresponds to the methyl proton of NpOH (1-NpOH, δ = 1.47 ppm; 2-NpOH, δ = 1.40 ppm; Figure 2). Only one doublet is observed for this methyl group in the presence of cyclodextrin, suggesting that the equilibration dynamics is fast. The position for the chemical shift of this doublet is determined by the average environment sensed by NpOH taking into account the fraction of bound and free probe. Two doublets are observed for racemic 1-NpOH is the presence of β-CD (inset Figure 2). This observation can be explained either by different equilibrium constants or different $\Delta\delta_{max}$ values for each enantiomer.

The values for $\Delta\delta$ of the NpOH methyl proton at different β-CD concentrations were obtained in three independent experiments for each enantiomer of 1-NpOH and 2-NpOH. The variation of $\Delta\delta$ with β-CD concentration for all independent experiments with each enantiomer were combined and were fitted to eq 1 (Figure 3). For both NpOHs the double-reciprocal plots were linear (inset Figure 3), which is consistent with a 1:1 stoichiometry for the complex. The K_{eq} values for both NpOHs determined by ^{1}H NMR (Table 2) are similar to those determined by fluorometry. The $\Delta\delta_{max}$ values are different for each enantiomer of 1-NpOH and 2-NpOH, suggesting that each enantiomer experiences a different environment within the chiral cyclodextrin. This is expected since the complexes of enanti-

TABLE 2: Equilibrium Constants and Maximum Shifts for the Complexation of NpOHs with β-CD Determined by ^{1}H NMR[a]

compd	$K_{eq}/10^3$ M^{-1}	$\Delta\delta_{max}$/ppm
(*R*)−1-NpOH	0.23 ± 0.01	0.047 ± 0.001
(*S*)−1-NpOH	0.19 ± 0.01	0.056 ± 0.002
(*R*)−2-NpOH	0.82 ± 0.09	0.034 ± 0.001
(*S*)−2-NpOH	1.0 ± 0.2	0.020 ± 0.001

[a] Errors correspond to those recovered from the nonlinear fit to eq 1.

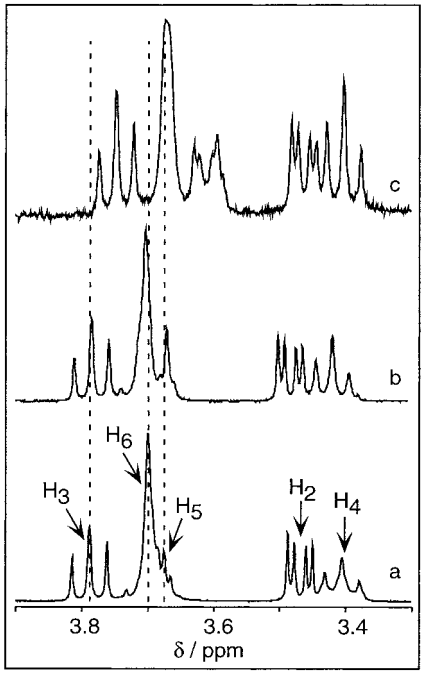

Figure 4. ^{1}H NMR spectra for β-CD in D_2O (a) and in the presence of (*R*)-1-NpOH ([β-CD] = 0.5 mM) (b) and (*R*)-2-NpOH ([β-CD] = 0.12 mM) (c).

omers with β-CD have a diastereomeric relationship, which can lead to different spectroscopic properties.

In addition to the determination of K_{eq} values, ^{1}H NMR can also provide information on the complexation geometry. Analysis of the shifts corresponding to the protons of β-CD can be related to the location of the guest in the cyclodextrin cavity. An upfield shift for the cyclodextrin protons is expected when an aromatic guest molecule is located close to the protons in question.[16] The glucose H_3 and H_5 protons are located within the cavity, whereas protons H_6 are located at the narrower entrances and protons H_2 and H_4 at the wider entrance. The assignment of the ^{1}N NMR signals of β-CD[17] is shown in Figure 4. The values for the chemical shifts for β-CD are shifted by ca. 0.2 ppm upfield compared to the published data,[17,20] which is probably due to slight differences in the procedure for signal referencing. In the presence of 2-NpOH (Figure 4c), the H_3, H_5, and H_6 β-CD signals shift by 0.05, 0.08, and 0.03 ppm, respectively. However, a much smaller shift (≤0.01 ppm) is observed for H_4 and H_2. This result suggests that 2-NpOH is axially incorporated into the β-CD cavity. In the presence of 1-NpOH, very small shifts (≤0.02 ppm) are observed for the cyclodextrin signals, and the magnitude for the shift for each cyclodextrin proton cannot be compared. For this reason, no information is available about the 1-NpOH position within the complex. The small shifts observed are a consequence of the smaller equilibrium constant for 1-NpOH complexation which leads to a small fraction (<10%) of complexed β-CDs. This

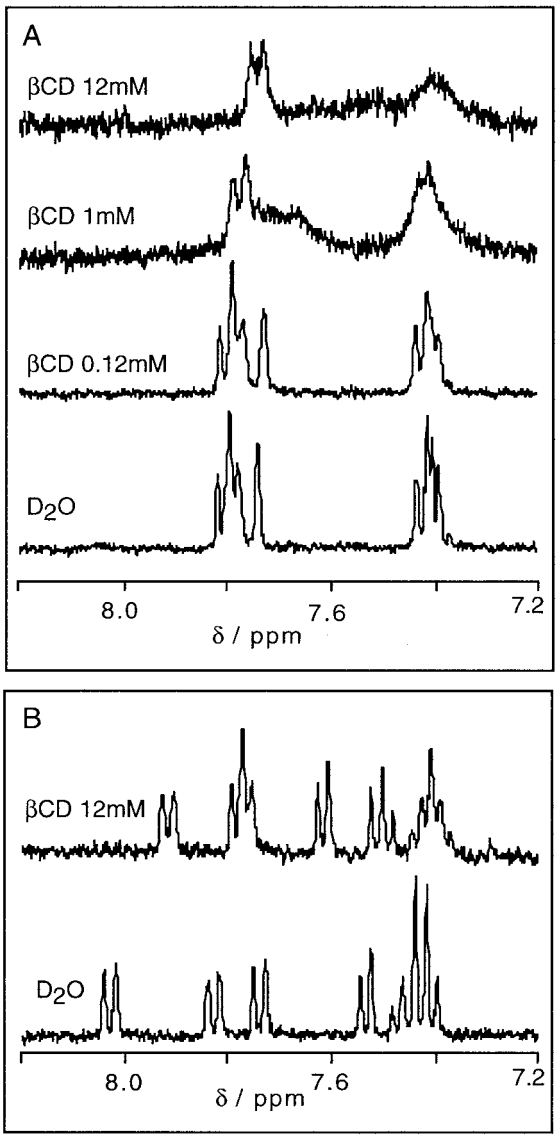

Figure 5. ^{1}H NMR spectra for the aromatic protons of 0.3 mM of (*R*)-2-NpOH (A) or (*R*)-1-NpOH (B) in the absence and presence of β-CD.

situation cannot be optimized since we have already reached the solubility limit for 1-NpOH.

The effect of β-CD complexation on the signals corresponding to the aromatic α- and β-protons of 1-NpOH and 2-NpOH are very different (Figure 5). In the case of 1-NpOH, all signals corresponding to the aromatic protons shift to some extent, but no significant broadening of the peaks is observed. In contrast, for 2-NpOH a significant broadening of the peaks is observed even at low β-CD concentrations. Broadening of ^{1}H NMR signals has been previously observed for naphthalene tethered cyclodextrins[18,43] and was ascribed to dynamic effects. Broadening of the NMR signal indicates the occurrence of a slow exchange process. As will be shown below, this processes is assigned to the dynamics of the 2:2 β-CD/2-NpOH complex.

Calorimetry was the third technique employed to determine the equilibrium constant values. The binding isotherms for each enantiomer of 1- and 2-NpOH were determined at various temperatures (14−36 °C). No heat release was observed when β-CD was injected into pure water. The heat release for each injection of β-CD was typically below 0.5 and 1.5 μcal/s for 1- and 2-NpOH, respectively. These values are below the specified detection limit of the equipment (2 μcal/s). The equilibrium

constants for each enantiomer were recovered by assuming a 1:1 complexation stoichiometry, and the recovered values had errors of up to 30%. In addition, in the case of 2-NpOH, the plots for the free energy as a function of temperature were very scattered. For this reason, we chose to estimate an average equilibrium constant at 20 °C by taking into account all data at different temperatures. The estimated values are $(6 \pm 1) \times 10^2$ M^{-1} and $(7 \pm 2) \times 10^2$ M^{-1} for (*R*)- (14 determinations) and (*S*)-2-NpOH (13 determinations), respectively. The equilibrium constant for (*S*)-2-NpOH in D_2O (4 determinations) was estimated to be $(8 \pm 2) \times 10^2$ M^{-1}. In the case of 1-NpOH, the value for the equilibrium constant is $(1.6 \pm 0.3) \times 10^2$ M^{-1}. The values for the equilibrium constants determined by calorimetry are somewhat lower than those obtained from ^1H NMR and fluorometry data. However, taking into account the errors associated with the calorimetry data, the agreement between the techniques is adequate. It is worth noting that the equilibrium constants did not vary significantly if the experiments were performed in water or D_2O. This is a very important observations since it indicates that the NMR and fluorometry data can be compared.

Dynamics of Triplet NpOH Complexation to β-CD. Triplet-excited 1-NpOH and 2-NpOH have the same absorption spectra as naphthalene which is characterized by a sharp absorption peak between 410 and 420 nm.[44] All triplet decays were measured at 420 nm. NpOHs are easily photoionized in aqueous solution, leading to the observation of solvated electrons, which absorb above 600 nm, and a residual long-lived absorption below 450 nm, which is probably due to NpOH radical cations. The contribution from solvated electrons was minimized by attenuating the laser power. However, no significant change was observed for the triplet lifetime in the presence and absence of photoionization. We were not always able to maintain an adequate signal-to-noise ratio and completely eliminate the photoionization process. For this reason, in some experiments the decay at 420 nm had a long-lived residual which was taken into account when obtaining the values for the triplet lifetimes.

The triplet-excited lifetimes for 1-NpOH and 2-NpOH in aqueous solution were longer than 30 μs and were limited by the presence of small amounts of solvent impurity or residual oxygen. In the presence of 12 mM β-CD, the triplet decay followed a first-order process and the lifetimes for both NpOHs increased significantly. This increase is due to complexation to the cyclodextrin cavity, which can diminish the intrinsic decay rate constant but can also protect the chromophore from quenchers in solution.

The triplet−triplet absorption spectra of naphthalenes are the same in solvents of different polarity. Consequently, the dynamics of complexation of triplet NpOH cannot be measured directly, and the quenching methodology was employed.[29] Conceptually, in this methodology a molecule is used which primarily quenches the triplet probe in the aqueous phase. As the quencher concentration is increased, the exit of the probe from the cyclodextrin cavity becomes rate limiting and a curvature is expected for the quenching plot (k_{obs} vs [Q]). In most cases, the quencher also interacts with the triplet probe in the cavity, although with a lower quenching efficiency. For this reason, the quenching plots do not level off at high quencher concentrations but approach a linear relationship.[29] An ionic quencher (Mn^{2+}) was employed, since a higher quenching efficiency in the aqueous phase is desired compared to the quenching probability inside the cyclodextrin. The quenching plots for the triplet NpOHs by Mn^{2+} in water in the presence of 0.5 M SO_4^{2-} were linear, and the quenching rate constant

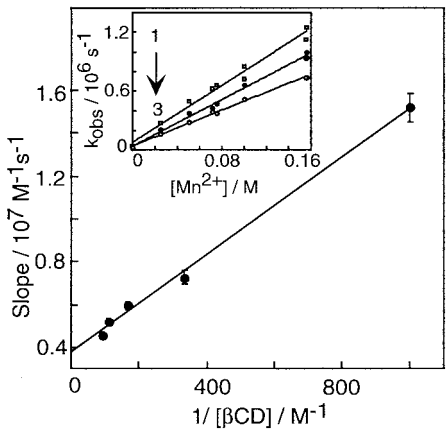

Figure 6. Dependence of the initial slope for the quenching plots of (*S*)-1-NpOH with the inverse of the β-CD concentration. The inset shows the quenching plot at low Mn^{2+} concentrations for various β-CD concentrations (**1**, 3 mM; **2**, 6 mM; **3**, 11 mM).

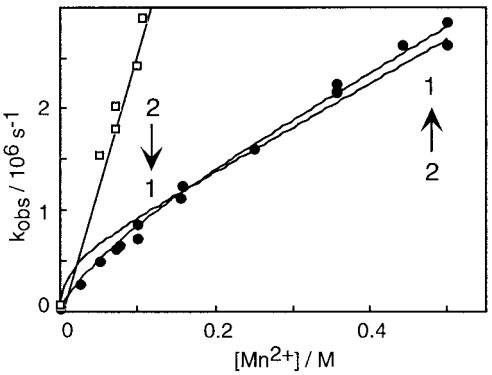

Figure 7. Quenching plot for (*S*)-1-NpOH by Mn^{2+} in water (□, only low Mn^{2+} concentrations shown) and in the presence of 3 mM of β-CD (●). The data in the presence of β-CD were fitted to eq 7 by fixing the parameters to the following values: $k_o = 4.7 \times 10^4$ s^{-1}; $k_H = 3.4 \times 10^4$ s^{-1}; $k_q = 2.6 \times 10^7$ M^{-1} s^{-1}; $k_q(H) = 4.3 \times 10^6$ M^{-1} s^{-1}. Two fits with different k_+ values (**1**, 8×10^8 M^{-1} s^{-1}; **2**, 1×10^8 M^{-1} s^{-1}) are shown.

was determined to be $(2.6 \pm 0.4) \times 10^7$ M^{-1} s^{-1}. Quenching of 1-NpOH was studied at various β-CD concentrations (2−12 mM), and at all quencher concentrations the triplet 1-NpOH decay was monoexponential. A value of $(4.3 \pm 0.4) \times 10^6$ M^{-1} s^{-1} (average of 3 determinations) was determined for k_q(H) from the dependence of the initial slope of the quenching plots with the inverse of the cyclodextrin concentration (eq 9, Figure 6). This value is only 5 times smaller than the quenching efficiency in water, and the small difference between the quenching efficiencies leads to quenching plots which are not very curved (Figure 7). Consequently, the recovered values for the entry and exit rate constant obtained by fitting the data to eq 7 have significant errors. Several fits were performed in which the values for k_+ were fixed and k_- was determined by employing eq 7 (Figure 7; see Experimental Section).[45] Figure 7 shows two fits, one of which leads to acceptable agreement with the experimental data and one which is inadequate. The errors for k_+ and k_- (Table 3) represent the extremes for the rate constant values for which adequate fits were observed. Within experimental errors the values for the entry and exit rate constants were the same for both enantiomers of 1-NpOH. Two other ionic quenchers, $[Co(NH_3)_5Cl]^{2+}$ and NO_2^-, were employed to establish if we could obtain larger differences for the quenching of triplet NpOH in water and when complexed to β-CD and, consequently, obtain better curvatures for the quenching plots. Although both molecules have higher quench-

TABLE 3: Entry and Exit Rate Constants for NpOHs for 1:1 Complexes with β-CD Determined from Quenching by Mn^{2+} [a]

compd	$k_+/10^8$ M^{-1} s^{-1}	$k_-/10^5$ s^{-1}
1-NpOH	4.7 ± 1.9 (7)	4.8 ± 1.8 (7)
2-NpOH	2.9 ± 1.6 (7)	1.8 ± 0.7 (7)

[a] The errors were estimated from fits with several fixed k_+ values (see text). The numbers in parentheses correspond to the number of independent experiments.

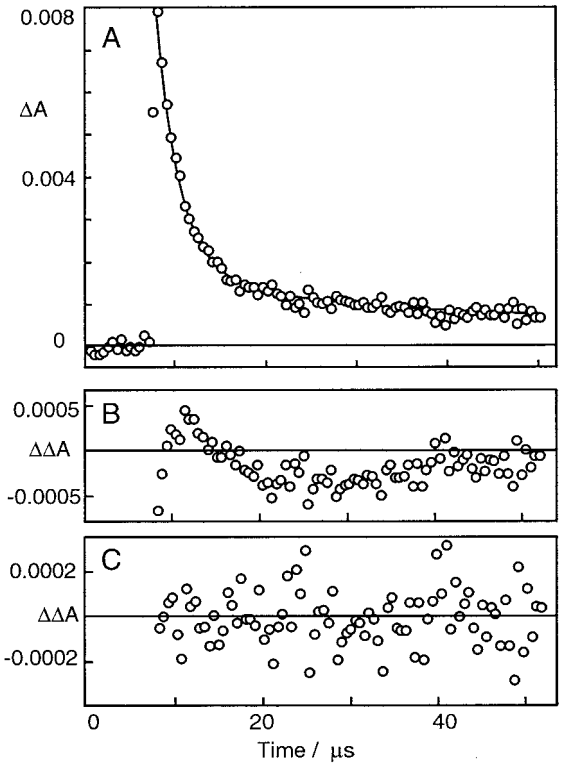

Figure 8. Decay of (*S*)-2-NpOH in the presence of 6 mM β-CD and 0.155 M Mn^{2+} (A). The solid line represents the fit to the sum of two exponentials. Panels B and C show the residuals for the fit to one and two exponentials, respectively.

ing efficiencies in water, no improvement was observed for the quenching plots in the presence of β-CD. In addition, analysis of a small set of the quenching plots with $[Co(NH_3)_5Cl]^{2+}$ and NO_2^- led to similar values for k_+ and k_- as recovered by using Mn^{2+} as a quencher.

In the case of 2-NpOH at 150 μM, a nonexponential fit was observed when the Mn^{2+} concentration exceeded 0.07 mM. This decay was adequately fitted to the sum of two exponentials (Figure 8). One possibility for this behavior is that the assumption made to derive eq 7, i.e., small free probe concentration, does not hold. In this case, the kinetic scheme would be similar to the dynamics of pyrene excimer formation where the decay always has two components.[29,46] However, the dependence of the observed rate constants for each exponential of the decay with quencher concentration does not follow the behavior expected for this latter kinetic scheme. In particular, the decrease of the triplet lifetime for the slow component is very small as the quencher concentration is increased. Since we observed the formation of 1:1 and 2:2 β-CD/2-NpOH complexes in the fluorescence studies, we assign the fast decay to the dynamics of the 1:1 complex and the slow decay to the processes involving the 2:2 complex. The fact that the second decay is only observable when the quencher concentration exceeds 0.07 mM suggests that the intrinsic

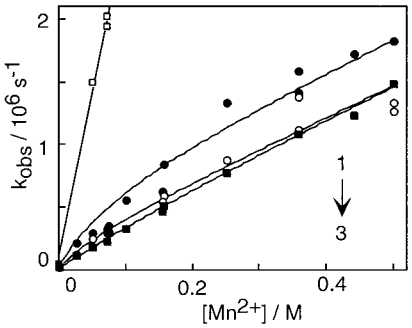

Figure 9. Quenching plot for (*R*)-2-NpOH in water (□, only low Mn^{2+} concentrations shown) and in the presence of β-CD (**1**, 3 mM; **2**, 6 mM; **3**, 12 mM).

lifetimes of 2-NpOH in the 1:1 and 2:2 complexes are very similar. In addition, when the 2-NpOH concentration was decreased to 10 μM, only monoexponential decays were observed for the triplet in the presence of β-CD (2 mM) and Mn^{2+} (between 0 and 0.5 M). This dependence of the number of exponentials on the 2-NpOH concentration is in line with the assignment of the slow decay to the 2:2 complex, since at low 2-NpOH concentrations only the complex with 1:1 stoichiometry is formed.

The dependence of the fast triplet decay of 2-NpOH (150 μM) in the presence of β-CD and Mn^{2+} follows the same pattern as observed for 1-NpOH (Figure 9). The value for k_q(H) obtained from eq 9 was (2.5 ± 1.7) × 10^6 M^{-1} s^{-1}. The entry rate constant is the same within experimental errors as that observed for 1-NpOH (Table 3), whereas the exit rate constant is smaller than for 1-NpOH.

Analysis of the slow component for the 2-NpOH decay is more difficult. A nonpulsed monitoring beam is employed to reliably measure lifetimes in the millisecond time domain. However, with a nonpulsed beam the signal-to-noise ratio decreases and leads to larger errors for the measured lifetimes. In addition, to have reasonable triplet signals, we always observed some photoionization of the 2-NpOH. For this reason, the absorption at 420 nm has a contribution from radical cations. At very long delays (ca. 1 ms) the transient spectrum is very broad and does not show the characteristic fine structure for the triplet absorption, suggesting the presence of weakly absorbing but long-lived transients. Since the magnitude for the absorption related to the slow component is small, it is very important to determine at which delay all the triplet has decayed, so that accurate lifetimes can be measured. The value for the residual absorbance at long delays was determined in the absence of quencher, and this residual absorbance was employed for all the fits. The lifetime for the fast component was determined for measurements over short periods of time, and this values was employed as a fixed parameter for the fit to two exponentials at longer times, where most of the decay corresponds to the slow component. It is important to note that despite the difficulties described, the experimental approach employed leads to an *estimate* of the dynamics for the 2:2 complex.

Within the experimental error the quenching plots for the slow component are linear (Figure 10A). Mn^{2+} is a much less efficient quencher for triplet 2-NpOH in the 2:2 complex than observed for the 1:1 complex, suggesting that the probe in the 2:2 complex is much better protected from aqueous quenchers. The slope of the quenching plots (Figure 10A) shows only a small dependence with the inverse of the β-CD concentration (Figure 10B). These data can be employed to estimate the value for k_q(H) and k_- for the 2:2 complex. The intercept corresponds

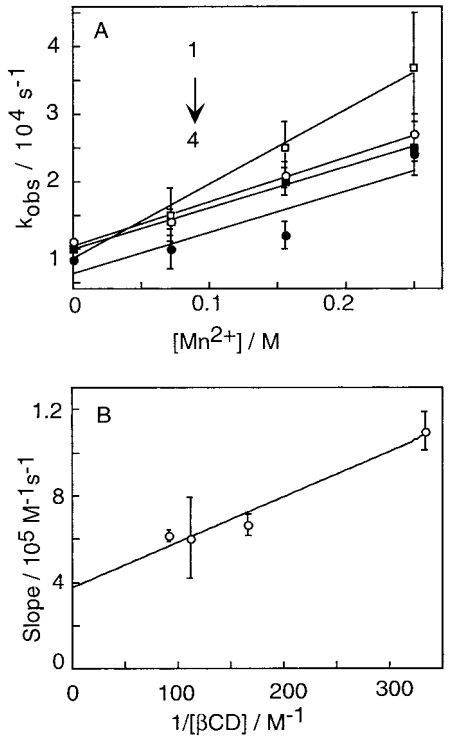

Figure 10. A: Quenching plots for the slow component of (*S*)-2-NpOH in the presence of β-CD (**1**, 3 mM; **2**, 9 mM; **3**, 6 mM; **4**, 11 mM). B: Dependence of the slope for the quenching plots with the inverse of the β-CD concentration.

to k_q(H), and its value was estimated to be $(3.7 \pm 0.6) \times 10^4$ M^{-1} s^{-1}, which is ca. 700 and 70 times smaller than observed for the quenching of 2-NpOH water and in the 1:1 complex, respectively. The slope for the plot in Figure 10B is 210 s^{-1} which combined with the k_q value in water (2.6×10^7 M^{-1} s^{-1}) leads to a k_-/k_+ ratio of 8.1×10^{-6} M. It is very unlikely that the association rate constant for the 2:2 complex is higher than that observed for the 1:1 complex (3×10^8 M^{-1} s^{-1}). For this reason, the dissociation rate constant for the 2:2 complex has to be equal or smaller than 2.4×10^3 s^{-1}.

Discussion

Ground-State Complexation Efficiency. When the dynamics of host−guest complexation is studied, it is always necessary to determine the ground-state equilibrium constants, since the magnitude of this constant will determine the fraction of bound probe in the dynamic studies. In addition, studies of the ground-state equilibration yield information on the stoichiometry and structure. We employed ^{1}H NMR, fluorometry, and calorimetry to determine the equilibrium constant values. Calorimetry data yielded qualitative information since the recovered values for K_{eq} have large errors. However, this technique was instrumental to establish that the K_{eq} values are similar in water and D_2O. Consequently, the values determined by fluorometry and ^{1}H NMR can be compared.

Analysis of the double-reciprocal plots for the ^{1}H NMR and fluorometry experiments with 1-NpOH show that only a 1:1 complex with β-CD is formed. This complexation stoichiometry is also substantiated by the lack of any excimer emission. In addition, the recovered K_{eq} values from both techniques are very similar. The K_{eq} values obtained from fluorescence for the enantiomers of 1-NpOH are the same within the experimental errors, although the measured values for (*R*)-1-NpOH were always higher than those obtained for (*S*)-1-NpOH. However, from the ^{1}H NMR data a more efficient binding is observed for (*R*)-1-NpOH ($K_{eq}(R)/K_{eq}(S) = 1.21 \pm 0.08$). Besides this small chiral discrimination for the equilibrium constant values, a difference was also observed for the $\Delta\delta_{max}$ values for both enantiomers, indicating that the perturbation by the chiral environment of the cyclodextrin is different for each enantiomer. The equilibrium constants for the 1:1 complexes of 1-methyl- (340 ± 40 M^{-1}) and 1-ethylnaphthalenes (630 ± 70 M^{-1}) with β-CD[26] are higher than the value observed for 1-NpOH. The binding efficiency of guests to cyclodextrin cavities is determined by the guest's size, dipolar character, and ability to accept hydrogen bonds.[47] The lower K_{eq} value for 1-NpOH is probably due to the higher dipolar character and hydrogen-bonding accepting capability of this guest which contains a hydroxyl group when compared to the alkylnaphthalenes. The formation of a 2:2 complex, in addition to the 1:1 complex, was proposed for the 1-methyl- ($K_2 = 5820$ M^{-1}) and 1-ethylnaphthalene complexation with β-CD.[26] However, for 1-NpOH we do not have any evidence for the formation of such a complex, since no excimer emission was observed and the double-reciprocal plots were always linear. Unfortunately, the low complexation efficiency of 1-NpOH precluded the determination of which ^{1}H NMR signals of the cyclodextrin have a larger shift when the guest is complexed, and no information on the structure of the complex could be obtained.

Analysis of the complexation behavior for 2-NpOH shows the importance of using complementary techniques, since fluorometry led to the correct complexation stoichiometries, whereas NMR spectroscopy provided information on the structure of the complexes. The presence of the 2:2 complex is clearly established in the fluorescence studies, where a nonlinear double-reciprocal plot and an excimer emission were observed at high 2-NpOH concentrations. However, taken in isolation, the nonlinear fit to the monomer emission at high 2-NpOH concentrations led to an adequate fit but an incorrect K_1 value. This result shows that analysis of double-reciprocal plots are essential to ensure that the assumed stoichiometry is correct. In the case of fluorescence, the double-reciprocal plot is very sensitive to the formation of the 2:2 complex, because it leads to an apparent decrease of the monomer emission quantum yield. In contrast, from the ^{1}H NMR data no significant deviation from linearity was observed in the double-reciprocal plot, suggesting that the $\Delta\delta_{max}$ values for the methyl group in the 1:1 and 2:2 complexes are similar. Consequently, any deviation from linearity would only be perceptible if the values for K_1 and K_2 are very different, which is not the case for 2-NpOH. It is worth noting that the recovered equilibrium constants from the ^{1}H NMR data are the same, within experimental errors, as the K_1 values determined by fluorescence. This coincidence is fortuitous and again reflects the small differences between K_1 and K_2. However, the relative errors for the equilibrium constant values recovered from ^{1}H NMR data are much larger for 2-NpOH than for 1-NpOH, which suggests the interference of the 2:2 complex in this measurement.

Although ^{1}H NMR was not very suitable to measure the equilibrium constants for 2-NpOH, it provided important information on the structure of the complex. Analysis of the changes caused by complexation on the signals for the cyclodextrin protons suggests that 2-NpOH penetrates into the β-CD cavity as shown by the relatively large shifts for the H_3 and H_5 protons. In addition, the large shift observed for the H_6 protons, which are located at the narrower entrance of the cyclodextrin, suggests that a portion of the 2-NpOH molecule is located at

this entrance of the cavity. This is an interesting observation since most cartoon representations for cyclodextrin host−guest complexes show the inclusion of the guests from the wider entrance. We cannot differentiate at which end of the cyclodextrin the 2-NpOH hydroxyl group is located. This information would suggest from which entrance the association occurs. However, the complexation close to the narrow entrance indicates that the region defined by the cyclodextrin methylene groups should be viewed as an integral part of the cavity, and it could provide a more hydrophobic binding environment than at the wider entrance.

The K_1 value (800 ± 20 M^{-1}) for the complexation of 2-NpOH with β-CD is smaller than the values observed for 2-methyl- (1190 ± 40 M^{-1}) and 2-ethylnaphthalene (2000 ± 200 M^{-1}).[26] This behavior parallels that observed for 1-NpOH and suggests that the same factors lead to the smaller complexation efficiency for both NpOHs. It is interesting to note that the ratio of the K_1 values for naphthalenes substituted at the 2- and 1-positions is fairly constant (3.2−4.2) for the derivatives discussed above. This suggests that naphthalenes substituted at the 1-position are too spherical to fit into the β-CD cavity, whereas the more cylindrical 2-substituted naphthalenes can penetrate into the cavity.

Excimer emission, which indicates the formation of the 2:2 complexes, was observed for 2-methyl- and 2-ethylnaphthalenes. The values for K_2 are 1400 and 3370 M^{-1}, respectively.[26] However, no errors were reported, suggesting that the same softness to the fits was observed as we encountered for 2-NpOH. Any comparison of the magnitude of the K_2 values is not warranted, since the experimental errors are large. In any event, the fact that the values for K_2 are always higher than those observed for K_1, suggests that formation of 2:2 complexes is an efficient process.

The detailed studies related to the ground-state complexation of NpOHs with β-CD were performed in the absence of salts. We realized during our dynamic studies that high concentrations of $MnSO_4$ were necessary to obtain meaningful quenching data. For this reason, the K_1 and K_2 values were determined by fluorometry for both NpOHs with β-CD in the presence of 0.5 M Na_2SO_4. A significant increase was observed for K_1 for both NpOHs. In contrast, the K_2 value for the 2:2 complex formation with 2-NpOH was not very sensitive to the presence of salt. Although the effect of electrolytes on the equilibrium constants between guests and cyclodextrins has been reported,[48,49] the nature of this effect is not completely understood. A full characterization of the salt effect on cyclodextrin equilibrium constants is beyond the scope of this work. The absolute values for K_1 will only be important for the quantitative discussion below related to the complexation dynamics of triplet NpOHs.

Dynamics for the 1:1 NpOH/β-CD Complexes. The quenching experiments had to be performed at different β-CD concentrations in order to recover entry and exit rate constant values with reasonable errors. In addition, the fact that similar k_+ and k_- values are recovered for experiments at different β-CD concentrations verifies that the assumptions made when employing eq 7 were reasonable. The large errors for the dynamic parameters are a consequence of the small difference between the quenching efficiencies for the probe in water and when complexed to the β-CD. In the future, it will be desirable to establish what structural parameters are important for the quencher molecules to have a smaller quenching efficiency for the bound probe.

The quenching methodology has been previously employed to estimate the values for the entry and exit rate constants of triplet naphthalene with β-CD.[24] The value of 1×10^5 s^{-1} for the exit process compares well with the value determined for 2-NpOH (Table 3), as expected for molecules with similar inclusion modes. We cannot comment on the lower k_+ value measured for naphthalene, since no experimental details and errors were provided.[24] The entry and exit rate constants for 1-bromonaphthalene from β-CD at 15 °C were determined to be $(7 \pm 4) \times 10^7$ M^{-1} s^{-1} and $(6 \pm 3) \times 10^3$ s^{-1}, respectively, and the $k_q(H)/k_q$ ratio was determined to be ca. 1000.[31] Besides the difference in temperature, two additional factors may contribute for the much slower dynamics for 1-bromonaphthalene when compared to that for the NpOHs. (i) The experiments with 1-bromonaphthalene were performed in the presence of 10% acetonitrile, which lead to an enhancement of the complexation efficiency. With respect to dynamic aspects, the addition of alcohols as cosolvents have been shown to significantly decrease the exit rate constant when xanthone is complexed to β-CD.[34] A similar effect could be occurring for the 1-bromonaphthalene dissociation. (ii) The dynamics for 1-bromonaphthalene and β-CD could be related to a 2:2 complex and would for this reason not be a good comparison for the 1-NpOH dynamics.

The entry and exit processes for [*n*-(4-bromonaphthoyl)alkyl]-trimethylammonium bromide with α-, β-, and γ-CD are slower than observed for the NpOHs,[20] suggesting that the size of the guest molecules affects the complexation dynamics. The entry rate constants for these naphthalene derivatives were not very sensitive to the size of the alkyl chain and the cyclodextrin cavity. However, the exit rate constant is very sensitive to the guest and host structures. For example, for the naphthalene derivative with a long alkyl chain complexed to γ-CD, the decay in the presence of quencher showed a two exponential decay, which was assigned to two complexes with different structures where one of them is better protected from quenchers in the aqueous phase.[20] In this respect, this two exponential decay resembles the kinetics observed for 2-NpOH at high concentration, which we assigned to the dynamics of the 1:1 and 2:2 complexes.

The dynamics of the triplet NpOHs can be compared to that of triplet xanthone. The entry rate constants of both NpOHs are similar to that observed for xanthone ($(4 \pm 1) \times 10^8$ M^{-1} s^{-1}).[33] These rate constants are about 1 order of magnitude smaller than the diffusional rate constant in aqueous solutions. However, k_+ may be close to the diffusion-controlled limit taking into account geometrical factors, since formation of the complex needs the achievement of a specific geometry between the guest and the entrance of the cyclodextrin cavity. For example, the collision of the guest with the side walls of the cyclodextrin is unlikely to lead to the formation of a complex. The achievement of this specific geometrical arrangement will lead to a decrease for the diffusional rate constant associated with the complex formation process. Alternatively, the insensitivity of the association process to the structure of the guest could indicate that the rate-limiting step for entry is related to an intrinsic process of the cyclodextrin, such as disolvation of its cavity.

The analysis of the K_1 values and the ^1H NMR data for 1-NpOH and 2-NpOH suggests that 2-NpOH is located within the cyclodextrin cavity, whereas 1-NpOH may only be interacting with the rim of β-CD. These different complexation sites could be responsible for the 2.5 times higher exit rate constant observed for 1-NpOH. In comparison, the exit process for triplet xanthone is much faster ($(8.4 \pm 0.7) \times 10^6$ s^{-1}),[33] suggesting that either the location of xanthone within the complex or some

other fundamental property of triplet xanthone is very different from that for the NpOHs. The location of xanthone within the complex is probably not responsible for the higher k_- values, since its ground-state equilibrium constant with β-CD (1100 ± 200 M^{-1})[33] is higher than that observed for the NpOHs. Assuming that the insensitivity of the k_+ values also occurs in the ground state, this higher K_1 value would indicate a slower dissociation of the xanthone ground state when compared to the NpOHs, suggesting that xanthone is not loosely bound to β-CD. The fast exit of xanthone has been suggested to be due to the higher dipole moment of its π,π^* triplet state.[32] However, this trend would also be expected to occur to some extent for the NpOHs since their triplet states have the same configuration. The equilibrium constants for triplet xanthone, 1-NpOH, and 2-NpOH can be calculated from the ratio of k_+ over k_-, and these constants have values of $(5 \pm 1) \times 10$, $(1.0 \pm 0.5) \times 10^3$, and $(2 \pm 1) \times 10^3$ M^{-1}, respectively. Although the errors for the NpOH triplet equilibrium constants are large, as a consequence of the relatively large errors for the rate constants, it is clear that if any decrease occurs for these NpOH triplet equilibrium constants it is much less pronounced than the decrease by a factor of 20 observed in the case of xanthone. Linear solvation free energy relationships[50] have been employed to rationalize the complexation of guests in organized structures, such as cyclodextrins[47] and micelles.[51] In the case of micelles, it was shown that the dipolarity parameter, which would be related to the higher dipole moment of the excited state, is negligible when defining the binding efficiencies of solutes, and for solutes of the same size only the hydrogen-bonding ability is important.[51] However, for complexation of guests to β-CD a smaller dipolarity and hydrogen-bonding ability enhance the binding efficiency.[47] The remarkable difference for the k_- values of the NpOHs and xanthone could be explained if, for triplet xanthone, both an increase of its dipole moment and its hydrogen bonding ability are responsible for the increase of the k_- value. Clearly, any generalization for the behavior of the complexation dynamics is premature since not enough examples are known to differentiate between the factors that affect the entry and exit processes of guest molecules with cyclodextrins.

Finally, it is worth noting that the fact that no chiral discrimination was observed for the recovered entry and exit rate constants does not mean that such a discrimination does not occur but is a consequence of the large errors for the recovered k_+ and k_- values. On the basis of the small discrimination observed for K_1 for the enantiomers of 1-NpOH and β-CD, we would expect any differences for the entry and exit rate constants to be smaller than our experimental errors. For this reason, the assessment if chiral discrimination occurs in the dynamics of complexation will have to wait until better quenchers or chiral probes for direct kinetic studies are developed.

Dynamics for the 2:2 β-CD/2-NpOH Complex. The formation of the 2:2 complex is demonstrated by the excimer emission that is observed only at high 2-NpOH concentrations. In the absence of quencher, the NpOH triplet decay follows a monoexponential decay suggesting that the triplet lifetime is the same for the probe incorporated into 1:1 and 2:2 complexes. This observation eliminates an efficient self-quenching process in the 2:2 complex, since a shortening of the triplet lifetime would be expected if such a process was operating.

The quenching by Mn^{2+} for 2-NpOH in the 2:2 complex is much less efficient than the quenching observed for triplet NpOH in water and when included in the 1:1 complex. This protection is probably due to the encapsulation of the probe by two cyclodextrin molecules. For the quencher to access the probe in such an encapsulation it would have to penetrate into the cyclodextrin cavity from the opposite entrance. In contrast, the 1:1 complex always leaves part of the probe molecule exposed to the aqueous phase and the quencher only has to interact with the rim of the cyclodextrin in order to react with the triplet state.

Our study provides the *first estimate* for the rate constant related to the dissociation process of a cyclodextrin 2:2 complex. Since the exit of 2-NpOH from the 1:1 complex is fast (vide supra), it is reasonable to assume that the rate-limiting step for the dissociation of the 2:2 complex is the break-up of the cyclodextrin dimer. From the kinetics related to the triplet decay we estimated an upper limit for this dissociation rate constant ($k_- \leq 2.4 \times 10^3$ s^{-1}). NMR spectroscopy is instrumental in estimating a lower limit for k_-. Figure 5 shows that some of the aromatic peaks of 2-NpOH broaden in the presence of β-CD, whereas such an effect is not observed for 1-NpOH. Broadening indicates that the complexation dynamics is not under fast exchange on the NMR time scale, and the broadening for 2-NpOH was assigned to the formation of the 2:2 complex.

In a simplified manner, the exchange rate constant (k_{ex}) is related to the difference in the frequency ($\Delta\nu$) of two isomeric protons,[52] which in our case corresponds to the protons for the probe free in solution and complexed to β-CD. The transition between slow- and fast-exchange regimes for the NMR experiment takes place when

$$k_{ex} = \frac{\pi(\Delta\nu)}{\sqrt{2}} \tag{10}$$

If the entry and exit rate constants are larger than the k_{ex} value calculated from eq 10, the NMR measurements are under fast exchange and only an average signal is observed for each proton. In contrast, when the dynamics is slow compare to k_{ex}, two peaks are observed, one corresponding to the bound probe and another to the free probe. However, when the dynamics is close to the magnitude for k_{ex} broadening of the spectrum is observed.

The $\Delta\nu$ value for the methyl proton of 2-NpOH was obtained from the fit of the shift in the ^{1}H NMR signal with β-CD concentration ($\Delta\delta_{max} = 0.03$ ppm; $\Delta\nu = 10.8$ s^{-1}). Since only one peak was observed for this signal, the system is under fast exchange and the k_{ex} value calculated (24 s^{-1}) represents a lower limit for the exit rate constant. A further estimate can be obtained from the signals corresponding to the aromatic protons, for which broadening is observed. This broadening suggests that the $\Delta\nu$ values are larger than observed for the methyl protons, which is probably due to the interaction of the two aromatic rings in the 2:2 complex. Unfortunately, we do not have an exact value for $\Delta\nu$, and analysis of the shape of the signals is complicated by the presence of two complexes with different stoichiometries. We employed the shift of the broadened NMR signals to obtain an estimate for the exchange rate by making a conservative guess for the $\Delta\nu$ value. There are several peaks in the 7.75−7.8 ppm region that broaden. Some of these peaks appear to shift by more than 0.25 ppm since a broad shoulder is still observed at 7.5 ppm in the presence of 12 mM β-CD. The value of 0.25 ppm for a shift corresponds to a lower limit for the complexation dynamics of 200 s^{-1}.

On the basis of the kinetics for the triplet state and NMR analysis, we can estimate that the value for k_- will fall between 2×10^2 s^{-1} and 2.5×10^3 s^{-1}. As mentioned above, this rate

constant is probably related to the dissociation of the cyclodextrin dimer and this very slow dissociation rate constant for the 2:2 complex raises at least two intriguing mechanistic considerations. This slow dynamics could indicate that cyclodextrin solubilization in water does not lead only to cyclodextrins monomers, but many empty dimers or even higher oligomers could be present. Indeed aggregation of empty cyclodextrins has been proposed.[53] If empty oligomers exist, their presence would be important when cyclodextrins are used for self-assemblies or in supramolecular systems designed for a particular function, such as catalytic activity. Alternatively, the absence of 2:2 complexes for 1-NpOH may indicate that dimerization in the case of 2-NpOH is driven by the incorporated guest, which would be an example of a template effect. Obviously, both of the considerations above are speculative at this point, but they highlight how further studies to understand these slow dynamic processes involving more than one cyclodextrin molecule might have an impact on the use of cyclodextrins in supramolecular chemistry.

Conclusions

A detailed description of the complexation of NpOHs with β-CD and its entry and exit dynamics was achieved by employing complementary techniques which provide information on different aspects of the complexation behavior. The less efficient complexation of 1-NpOH when compared to 2-NpOH was expected on the basis of previous work with naphthalene derivatives. However, we observed the chiral discrimination for the binding of (*R*)- and (*S*)-1-NpOH with β-CD, although the degree of discrimination is small. Analysis of the dynamics for the 1:1 complexes for both NpOHs with β-CD showed that the exit process is much more dependent on the structure of the probes than the entry process. This is particularly noticeable when the NpOH dynamics is compared to that observed for xanthone. Finally, this work provides the first estimate for the dissociation rate constant of a 2:2 guest/cyclodextrin complex. The possibility of measuring these slow dissociation processes involving cyclodextrin dimers and possibly oligomers may prove important when using cyclodextrins as building blocks for supramolecular structures.

Acknowledgment. This research was supported by the Natural Sciences and Engineering Research Council of Canada, NSERC (C.B.), and the German Research Foundation, GRF (J.F.H.). C.B. thanks the Fritz-Haber Institut der Max-Planck Gesellschaft for partial financial support during her stay in Berlin. K.S. thanks NSERC for a Summer Student Research award, and T.C.B. thanks the Conselho Nacional de Desenvolvimento Científico e Tecnológico, CNPq (Brazil), for a postdoctoral fellowship. The authors thank L. Netter for support in software development, C. Greenwood for her assistance with the NMR experiments, and Cerestar for their kind gift of the cyclodextrin samples.

Supporting Information Available: Figures showing the change of the 1-NpOH fluorescence intensity with β-CD concentration and the correlation of changes in excimer intensity with β-CD concentration and the calculated excimer concentration and figures and tables providing two examples for the fitting of the triplet decays in the presence of quencher (6 pages). Ordering information is given on any current masthead page.

References and Notes

(1) (a) University of Victoria. (b) Fritz-Haber Institut der Max-Planck-Gesellschaft.

(2) Saenger, W. *Angew. Chem., Int. Ed. Engl.* **1980**, *19*, 344−362.

(3) Szejtli, J. *Cyclodextrins and their inclusion complexes*; Akadémiai Kiadó: Budapest, 1982.

(4) Szejtli, J. *Cyclodextrin Technology*, 1st ed.; Kluwer Academic Publishers: Dordrecht, The Netherlands, 1988.

(5) Szejtli, J.; Osa, T. *Cyclodextrins*; Elsevier Science Ltd.: New York, 1996; Vol. 3.

(6) Li, S.; Purdy, W. C. *Chem. Rev.* **1992**, *92*, 1457−1470.

(7) Szejtli, J. In *Cyclodextrins*; Szejtli, J., Osa, T., Eds.; Elsevier Science Ltd.: New York, 1996; Vol. 3, pp 5−40.

(8) Jicsinszky, L.; Fenyvesi, E.; Hashimoto, H.; Ueno, A. In *Cyclodextrins*; Szejtli, J., Osa, T., Eds.; Elsevier Science Ltd.: New York, 1996; Vol. 3, pp 57−188.

(9) Szejtli, J. In *Cyclodextrins*; Szejtli, J., Osa, T., Eds.; Elsevier Science Ltd.: New York, 1996; Vol. 3, pp 189−203.

(10) Fenyvesi, E.; Szente, L.; Russell, N. R.; McNamara, M. In *Cyclodextrins*; Szejtli, J., Osa, T., Eds.; Elsevier Science Ltd.: New York, 1996; Vol. 3, pp 305−366.

(11) Connors, K. A. *J. Pharm. Sci.* **1995**, *84*, 843−848 and references therein.

(12) Connors, K. A. *Binding Constants-The Measurement of Molecular Complex Stability*; John Wiley & Sons: New York, 1987.

(13) Connors, K. A. In *Cyclodextrins*; Szejtli, J., Osa, T., Eds.; Elsevier Science Ltd.: New York, 1996; Vol. 3, pp 205−241.

(14) Connors, K. A. *Chem. Rev.* **1997**, *97*, 1325−1357.

(15) Ramamurthy, V. *Photochemistry in Organized and Constrained Media*; VCH Publishers: New York, 1991.

(16) Demarco, P. V.; Thakkar, A. L. *Chem. Commun.* **1970**, 2−4.

(17) Muñoz de la Peña, A.; Ndou, T. T.; Zung, J. B.; Greene, K. L.; Live, D. H.; Warner, I. M. *J. Am. Chem. Soc.* **1991**, *113*, 1572−1577.

(18) McAlpine, S. R.; Garcia-Garibay, M. A. *J. Org. Chem.* **1996**, *61*, 8307−8309.

(19) Hamai, S. *Bull. Chem. Soc. Jpn.* **1982**, *55*, 2721−2729.

(20) Turro, N. J.; Okubo, T.; Chung, C.-J. *J. Am. Chem. Soc.* **1982**, *104*, 1789−1794.

(21) Fujiki, M.; Deguchi, T.; Sanemasa, I. *Bull. Chem. Soc. Jpn.* **1988**, *61*, 1163−1167.

(22) Hamai, S.; Mononobe, N. *J. Photochem. Photobiol. A: Chem.* **1995**, *91*, 217−221 and references therein.

(23) Fraiji, E. K., Jr.; Cregan, T. R.; Werner, T. C. *Appl. Spectrosc.* **1994**, *48*, 79−84.

(24) Hashimoto, S.; Thomas, J. K. *J. Am. Chem. Soc.* **1985**, *107*, 4655−4662.

(25) Encinas, M. V.; Lissi, E. A.; Rufs, A. M. *Photochem. Photobiol.* **1993**, *57*, 603−608.

(26) Hamai, S.; Hatamiya, A. *Bull. Chem. Soc. Jpn.* **1996**, *69*, 2469−2476.

(27) Hamai, S. *Bull. Chem. Soc. Jpn.* **1996**, *69*, 543−549.

(28) Harata, K.; Uedaira, H. *Bull. Chem. Soc. Jpn.* **1975**, *48*, 375−378.

(29) Kleinman, M. H.; Bohne, C. In *Organic Phtochemistry: Molecular and Supramolecular Photochemistry*; Ramamurthy, V., Schanze, K., Eds.; Marcel Dekker: New York, 1997; Vol. 1, pp 391−466.

(30) Rohrbach, R. P.; Rodriguez, L. J.; Eyring, E. M.; Wojcik, J. F. *J. Phys. Chem.* **1977**, *81*, 944−948.

(31) Turro, N. J.; Bolt, J. D.; Kuroda, Y.; Tabushi, I. *Photochem. Photobiol.* **1982**, *35*, 69−72.

(32) Barra, M.; Bohne, C.; Scaiano, J. C. *J. Am. Chem. Soc.* **1990**, *112*, 8075−8079.

(33) Liao, Y.; Frank, J.; Holzwarth, J. F.; Bohne, C. *J. Chem. Soc., Chem. Commun.* **1995**, 199−200.

(34) Liao, Y.; Bohne, C. *J. Phys. Chem.* **1996**, *100*, 734−743.

(35) Mwakibete, H.; Crisantino, R.; Bloor, D. M.; Wyn-Jones, E.; Holzwarth, J. F. *Langmuir* **1995**, *11*, 57−60.

(36) Benesi, H. A.; Hildebrand, J. H. *J. Am. Chem. Soc.* **1949**, *71*, 2703−2707.

(37) Almgren, M.; Grieser, F.; Thomas, J. K. *J. Am. Chem. Soc.* **1979**, *101*, 279−291.

(38) The plots of ΔI vs [β-CD] with the fits to eq 1 as well as the double-reciprocal plots are shown in the Supporting Information.

(39) Birks, J. B. *Photophysics of Aromatic Molecules*; Wiley-Interscience: London, 1970.

(40) Ueno, A.; Tomita, Y.; Osa, T. *Chem. Lett.* **1983**, 1635−1638.

(41) Ueno, A.; Moriwaki, F.; Osa, T. *Tetrahedron* **1987**, *43*, 1571−1578.

(42) Figure S2 in the Supporting Information shows fits with different equilibrium constant values for the 2:2 complex.

(43) McAlpine, S. R.; Garcia-Garibay, M. A. *J. Am. Chem. Soc.* **1996**, *118*, 2750−2751.

(44) Carmichael, I.; Hug, G. L. *J. Phys. Chem. Ref. Data* **1986**, *15*, 1−250.

(45) The Supporting Information contains representative tables for fits at various k_+ values and figures which show the fit to the experimental data.

(46) Cheung, S. T.; Ware, W. R. *J. Phys. Chem.* **1983**, *87*, 466−473.
(47) Park, J. H.; Nah, T. H. *J. Chem. Soc., Perkin Trans. 2* **1994**, 1359−1362.
(48) Park, H.-R.; Mayer, B.; Wolschann, P.; Köhler, G. *J. Phys. Chem.* **1994**, *98*, 6158−6166.
(49) Johnson, M. D.; Bernard, J. G. *Chem. Commun.* **1996**, 185−186.
(50) Abraham, M. H. *Chem. Soc. Rev.* **1993**, 73−83.
(51) Quina, F. H.; Alonso, E. O.; Farah, J. P. S. *J. Phys. Chem.* **1995**, *99*, 11708−11714.
(52) Sanders, J. K. M.; Hunter, B. K. *Modern NMR Spectroscopy: A Guide for Chemists*; Oxford University Press: New York, 1987.
(53) Miyajima, K.; Sawada, M.; Nakagani, M. *Bull. Chem. Soc. Jpn.* **1983**, *56*, 3556−3560.